Ultrasound in Med. & Biol. Vol. 16, No. 3, pp. 231–239, 1990
Printed in the U.S.A.

0301-5629/90 $3.00 + .00

Original Contribution

"SONOELASTICITY" IMAGES DERIVED FROM ULTRASOUND SIGNALS IN MECHANICALLY VIBRATED TISSUES

ROBERT M. LERNER,[†] S. R. HUANG[‡] and KEVIN J. PARKER[†,‡]
[†]Diagnostic Radiology and [‡]Electrical Engineering,
Rochester Center for Biomedical Ultrasound, University of Rochester, Rochester, NY 14627

(*Received* 3 *March* 1989; *in final form* 3 *October* 1989)

Abstract—A method has been developed for detecting and imaging the relative "stiffness," or elasticity of tissues. Externally applied vibration at low frequencies (10–1000 Hz) is used to induce oscillations within soft tissues, and the motion is detected by Doppler ultrasound. The results are displayed in a format resembling conventional Doppler color flow mapping, and are termed "sonoelasticity images." Preliminary experiments indicate that these novel images may be useful for detecting hard tumors in the prostate, liver, breast, and other organs.

Key Words: **Ultrasound, Tissue characterization, Doppler, Tumors, Prostate, Liver, Cancer.**

INTRODUCTION

Physicians have traditionally detected cancers by palpation which identifies abnormal regions of increased stiffness (elasticity, or hardness). The approach is currently limited to only those tumors which are accessible to palpation, and little quantitative data on tissue elastic properties exist. Gray scale ultrasound is insensitive to stiffness as an imaging parameter and often fails to reveal the full extent or existence of tumors which, upon pathologic examination are found to be palpably more stiff than surrounding, normal tissues.

Since not all lesions are amenable to palpation, a sensitive and objective method for imaging abnormal regional elasticity may improve detection of carcinoma and other disease processes such as liver fibrosis. We report progress on our preliminary experience with a method to incorporate tissue stiffness features into ultrasound images ("sonoelasticity") (Lerner and Parker 1987, 1988). The approach combines external mechanical stimulation of target tissues with Doppler ultrasound to map the relative tissue motion. The concept is that stiff tissues will respond differently to an applied mechanical vibration than normal tissues.

Recently, improved imaging has been accomplished by the application of a high resolution color Doppler ultrasound instrument as the vibration detector and display unit, rather than off-line computer reconstruction of range-gated Doppler data as was shown in our previous work (Lerner and Parker 1987). In this report, we present preliminary data on phantoms and excised specimens demonstrating this capability.

The application of a color Doppler blood flow instrument has theoretical limitations. Therefore, basic theory is presented as background to guide the interpretations of these preliminary results.

The mathematical treatment of Doppler shifts from time varying surfaces and objects in an inhomogeneous or layered medium is quite complex. The derivations involve linear and nonlinear terms, and are the subject of some controversy (Piquette et al. 1988; Censor 1988). A detailed analysis is beyond the scope of this paper, and may not be necessary for clinical interpretation of "sonoelasticity" images. The next section proceeds with simplifying assumptions to outline some fundamentals which are experimentally observed.

THEORY

Vibrating target in quiescent, homogeneous medium

The most important result of the simplified case is that the detected Doppler shift from sinusoidally vibrating objects is generally given by a Fourier-Bessel series of equally spaced harmonics above and below the Doppler carrier frequency (Holen et al.

1985). The detected signal is analogous to the FM broadcast spectrum of a pure tone.

To demonstrate this, we assume the signal backscattered from a stationary target insonified by an ultrasound signal at frequency ω_0 is given by:

$$s(t) = A \cos[\omega_0 t]. \tag{1}$$

In the case of a target, vibrating with velocity $v(t) = v_m \cos(\omega_L t)$ the instantaneous frequency of the received signal is assumed to be:

$$\omega_0 + \Delta\omega_m \cos(\omega_L t) \tag{2}$$

where ω_L is low frequency of the applied vibration (typically 20–1000 Hz), and $\Delta\omega_m$ is the maximum Doppler frequency shift, given by the well known Doppler equations:

$$\Delta\omega_m = \frac{2v_m\omega_0 \cos\theta}{c} \tag{3}$$

and where $\cos\theta$ is the angle between the vibration vector and the direction of insonification, and c is the speed of sound in the medium. For convenience, we assume the vibration is in the line with the Doppler insonification, and replace the $\cos\theta$ term with unity. Thus the received signal can be written:

$$s(t) = A \cos\left[\omega_0 t + \frac{\Delta\omega_m}{\omega_L} \sin(\omega_L t)\right]. \tag{4}$$

The instantaneous frequency of this expression, by definition the time derivative of the term in brackets, is thereby given by eqn (2). The cosine of a sine term can be represented by a trigonometric identity, so eqn (4) has a Fourier-Bessel series representation. The harmonics appear at $\pm N\omega_L$, where $N = 1, 2, 3 \cdots$. The harmonic amplitudes are given by (Carlson 1986):

$$s(t) = A \sum_{n=-\infty}^{\infty} J_n(\beta)\cos(\omega_0 t + n\omega_L t) \tag{5}$$

$$\beta = \frac{\Delta\omega_m}{\omega_L} = \frac{2v_m\omega_0}{\omega_L c} \tag{6}$$

where $J_n(\beta)$ is the Bessel function of the first kind of integer order n.

Since the tissue vibration velocity is the temporal derivative of displacement $\epsilon(t) = \epsilon_m \sin(\omega_L t)$, then $v_m = \omega_L \epsilon_m$ and the parameter β is directly related to tissue displacement as follows:

$$\beta = \frac{2\epsilon_m\omega_0}{c}. \tag{7}$$

In sonoelasticity imaging, the vibration velocity, the displacement, or β (all linearly proportional) may be measured and displayed as a function of position within tissues in order to detect regions of abnormal stiffness.

An important special case occurs when a very low frequency vibration is applied. Then a slowly varying single frequency Doppler shift may be observed on time-frequency displays as a sine wave instead of the theoretical Fourier-Bessel series result. This effect has been well demonstrated (Holen et al. 1985; Lerner and Parker 1988). Another important special case is that of inhomogeneous layered tissues, with different boundary vibration velocities at each interface. The topic is complex and has been considered elsewhere (Hermand et al. 1988) but the important theoretical result is that the measured Doppler shift from a deep region of interest may be influenced by vibrations in overlying tissues. The clinical application of this remains to be investigated in depth.

The estimation problem

We assume that range gated Doppler ultrasound from some region of interest produces a Fourier-Bessel series harmonic spectrum of the type indicated in eqns (5) and (6), with a typical example shown in Fig. 1. The task is to estimate the apparent velocity v_m, given a speed of sound and known ultrasound carrier frequency ω_0 and vibrational frequency ω_L. Note that $\Delta\omega_m$ (and therefore v_m) cannot be directly estimated from the observed harmonics, since the relationship between these is complicated (eqns 5 and 6), and one will only observe harmonics down to the instrument dependent electronic noise floor. Thus, a noisy and arbitrarily band limited or amplitude limited harmonic series must be used to determine β, and then $\Delta\omega_m$, and v_m.

The parameter β can be estimated by comparing the theoretical ratios of Bessel functions with the measured ratios of the amplitudes of the maximum and the second-maximum harmonics. This is likely to be more noise insensitive than the method of Yamakoshi et al. (1988) which compares first, second, and third (not necessarily the maximum) harmonics. Alternatively, the bandwidth of a tone-modulated FM signal can be approximated as $2\beta\omega_L$ (Carlson 1986). A problem with this simple approach is that the use depends on the instrument noise threshold and one's definition of "bandwidth." It is clear that new estimation algorithms will be required to accurately portray vibrations over an image field.

Although vibration produces a spectrum with zero mean Doppler shift, the color flow instruments generally display significant, non-zero mean Doppler shift due to the finite number of samples used in

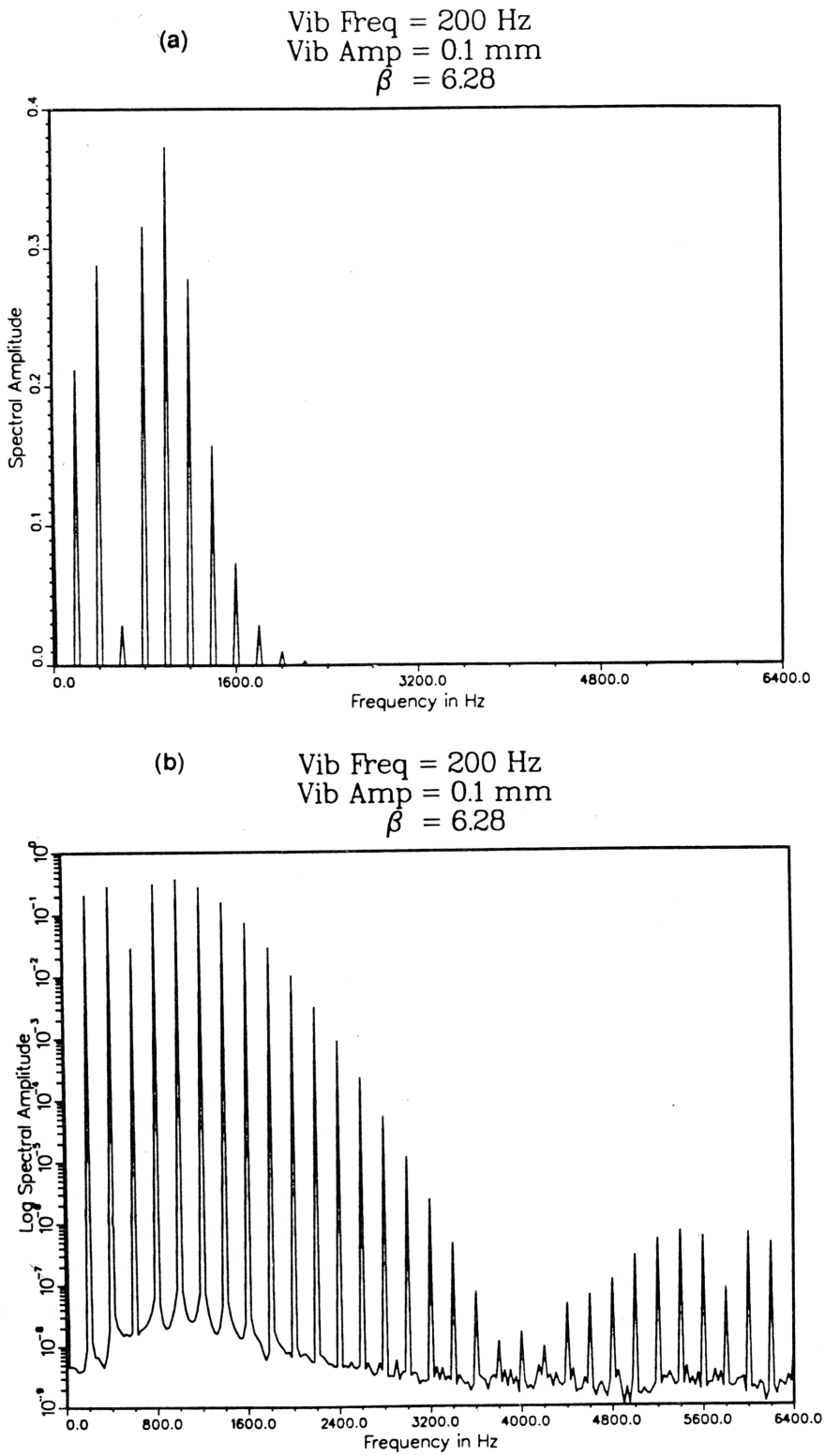

Fig. 1. Theoretical frequency domain representation of FM Doppler signal from 200 Hz vibrating target of with peak displacement of 0.1 mm, assuming an ultrasound carrier frequency of 7.5 MHz. The magnitude and spacing of harmonics follow a Fourier-Bessel series relation. In this case, the FM parameter β, is 6.28. Linear scale is shown in (a), log scale in (b).

estimation algorithms. Thus, although conventional Doppler flow mapping instruments are not optimized for the task of detecting vibrations, they can be utilized in a threshold sense as described in the next section.

METHODS

Phantoms were constructed to simulate hard and soft tissues. The phantoms were block shaped and were 5 to 10 cm on edge. The hard or stiff tumors were constructed from 3% agar, plus 1% gelatin in distilled water, with from 0.1% to 3% barium sulphate added for backscatter. Soft tissues were made from 1% agar, 1.5% gelatin with 1% barium sulphate mixed at 50°–70° C and degassed by vacuum during cooling and solidification. Elasticity was measured by a compression technique described in the companion paper (Parker et al. 1990). It was found that the stiff material had approximately five times the modulus of elasticity compared to the soft material. These phantom materials, and a rabbit liver containing VX2 carcinoma, and a prostate specimen from autopsy containing benign prostatic hyperplasia were examined *in vitro.* They were placed between anechoic gel pads with the low frequency acoustic vibration source placed below the lower gel pad and the color Doppler detector placed on the upper gel pad.

Vibrations were coupled to the specimens using an acoustic horn capable of output in the 20–1000 HZ audio band. A hard plastic cone (tapered down to a 4 mm opening) was coupled by light pressure to the base of phantoms or gel pads. At these low frequencies, the acoustic wave lengths are on the order of many centimeters and therefore, the source geometry should radiate as a point. Less than 10 watts electrical power was input to the acoustic source at all time, and the resulting vibrational amplitude at the point of contact was estimated, by observing the Fourier-Bessel spectra, to be less than 0.1 mm peak displacement at 200 Hz.

Images were made using a color Doppler instrument (Quantum, QAD1) at 7.5 MHz. This instrument was adjusted to display vibration in a threshold mode. Either blue or red (motion direction toward or away) indicated regions where the vibrational amplitude exceeded some threshold dictated by the gain (signal level) and Doppler threshold controls. The presence or absence of color was not dependant on B-scan reflectivity over a reasonable (greater than 30 dB) range. Thus, crude sonoelasticity images were obtained where presence of color indicated detected vibration above a combination of frequency shift (number of harmonics) and magnitude. In the results section red or white color represents the detection of at least one harmonic of 200 Hz vibration, at least 10 dB above noise floor. When vibration below threshold was present the instrument displayed only conventional gray scale information.

RESULTS

Sonoelasticity parameter estimation

Figure 1 shows a simulated typical spectrum of the received signal with the Bessel harmonics spaced 200 Hz apart, and $\beta = 6.28$. Figure 2(a) is simulated time-frequency display for constant frequency $f_L = 200$ Hz, varying the vibration amplitude $\epsilon_m = 0.03$ to 0.3 mm, left to center, then decreasing again to 0.03 mm center to right. Aliasing or foldover effects can be seen in the center region. These can be compared with the experimental results in Fig. 2(b) where the vibration amplitude was varied in approximately the same range. The number of significant Bessel harmonics increases as the vibration amplitude increases. Figure 3(a) is a simulated time-frequency display for constant amplitude $\epsilon_m = 0.1$ mm, varying the vibration frequency $f_L = 100$ Hz to 300 Hz left to

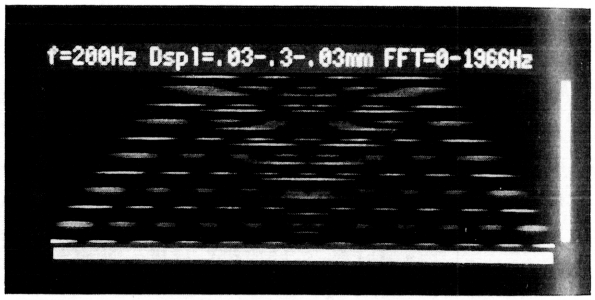

(a)

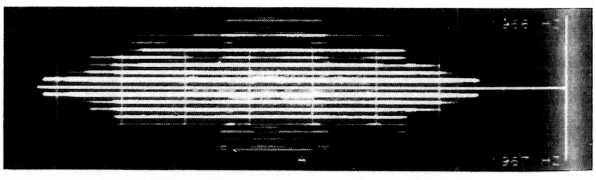

(b)

Fig. 2. Time-frequency display of the Doppler shift from 200 Hz vibration over a range of displacement amplitudes. Theoretical results are shown in (a) where the vertical scale is Doppler shift from 0 to 1966 Hz, and the horizontal scale represents different displacement amplitudes from 0.03 mm (left) to 0.3 mm (center) to 0.03 (right). In these cases the FM modulation parameter, β, varies from approximately 2 left to 19 center. In (b), experimental results from the Quantum QAD1 in Spectrum mode are given from a region of interest near a 200 Hz vibration source at "A," while the amplitude is varied from low to high to low (left to right on time-frequency display at bottom). The vertical spectral scale is −1967 to +1966 Hz Doppler shift.

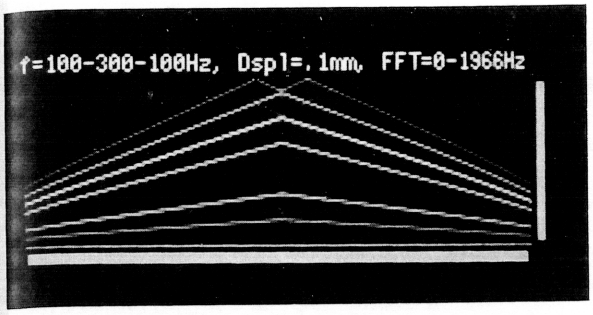

(a)

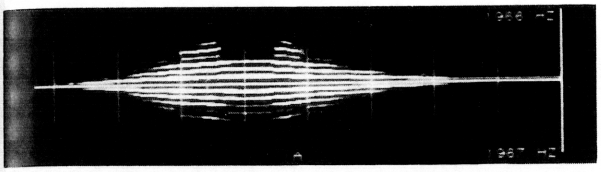

(b)

Fig. 3. Time-frequency display of the Doppler shift from a constant displacement but variable frequency object with an FM modulation parameter of $\beta = 6.28$. (a) Theoretical predictions for 0–1966 Hz Doppler shift (vertical scale), with vibrations ranging linearly from 100 Hz (left) to 300 Hz (center) and to 100 Hz (right). (b) A region near the acoustic vibration source analyzed as the source was slowly changed from 100 to 300 Hz. Since the horn could not maintain constant vibration amplitude over these frequencies, the number of harmonics shown is not constant, but the spacing between harmonics was observed to change proportional to vibration frequency.

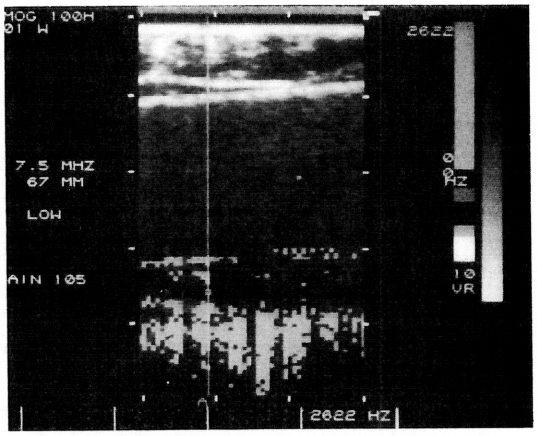

(a)

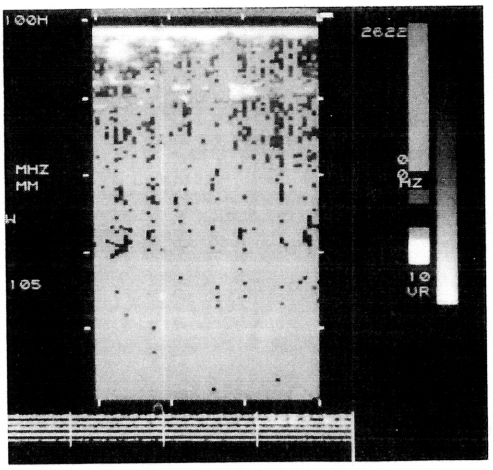

(b)

Fig. 4. Sonoelasticity image showing color "fill-in" over the B-scan image of a homogeneous phantom. In (a) the 200 Hz vibration source (at bottom) was at low amplitude, in (b) the source was increased by a factor of 5. The "fill-in" expanded upward with increasing source amplitude in a smooth fashion in the homogenous phantom.

center, then decreasing again to 100 Hz center to right. The spacing between harmonics increases as the vibration frequency increases, and aliasing is seen when harmonics occur at greater than the fold over frequency, 1966 Hz is this case. The experimental results in Fig. 3(b) show the results of varying vibration frequency, although we could not maintain constant amplitude over the range of frequencies, and this is manifested as the appearance of harmonics above display threshold.

Sonoelasticity imaging of phantoms and tissue

In Figs. 4–9 the imaging transducer is located at the top of the frame, and the vibration source at 200 Hz is applied through a plastic window to the bottom of the sample. Figures 4a and 4b show that in a homogeneous phantom, as the source amplitude is increased the color Doppler image fills-in from bottom to top in a reasonably homogeneous fashion. In contrast, Fig. 5(a) shows a hyperechoic, stiff wedge region embedded in a soft tissue phantom. When optimal vibration is applied, a clearly demarked color-free region corresponding to the stiff wedge is shown (Fig. 5b). In real-time the discrimination between regions is even more apparent, since the color within the stiff "tumor" appear randomly, whereas the fill in of surrounding soft tissues is consistent on a frame-to-frame basis. (Red color overlay appears as neutral gray blocks in the reproductions.)

An example using a cylindrical "stiff" hyperechoic region is shown in cross section where the Doppler fill-in is random and sporadic (on a frame by frame basis) within the "tumor," but consistent and more uniform in the surrounding soft material (Fig. 6). A number of tests on hypoechoic stiff regions produced similar results, thus the Doppler detection and fill-in is not related to backscatter strength over a wide range of target echogenicity.

Figure 7(a) shows a rabbit liver *in vitro* containing 2 cm VX2 tumor. The liver is sandwiched be-

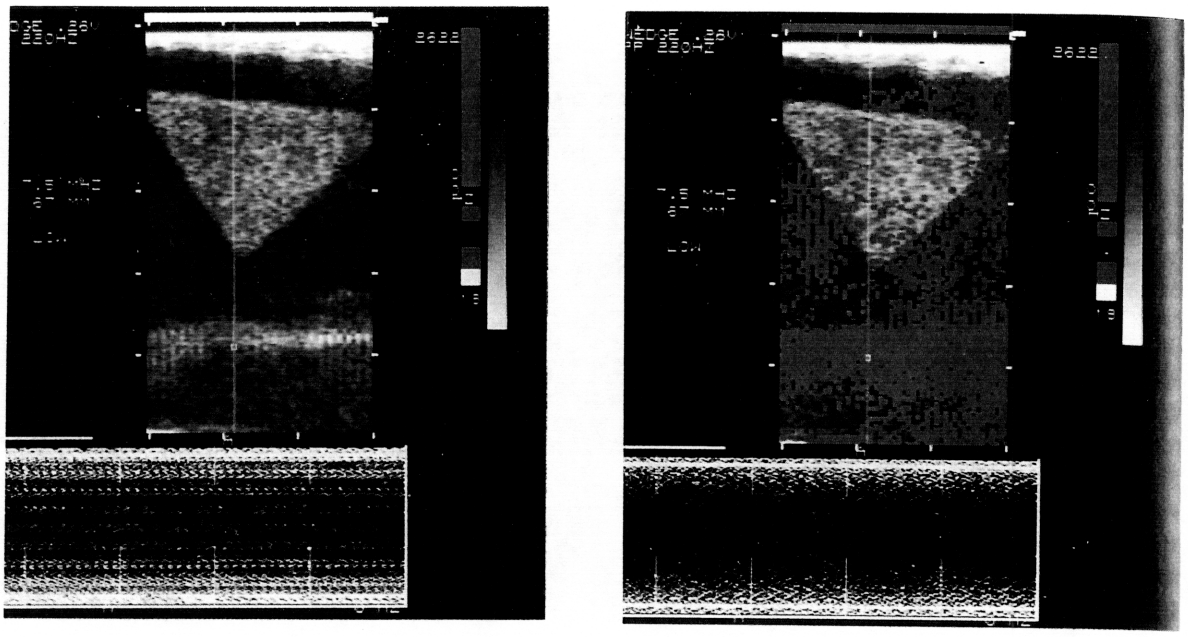

(a) (b)

Fig. 5. Image of a "soft" phantom containing a "stiff" wedge. (a) Conventional B-scan image. (b) Sonoelasticity image exhibiting Doppler fill-in of regions in which vibration is detected. The detected vibration outlines the soft medium but not the stiff "tumor."

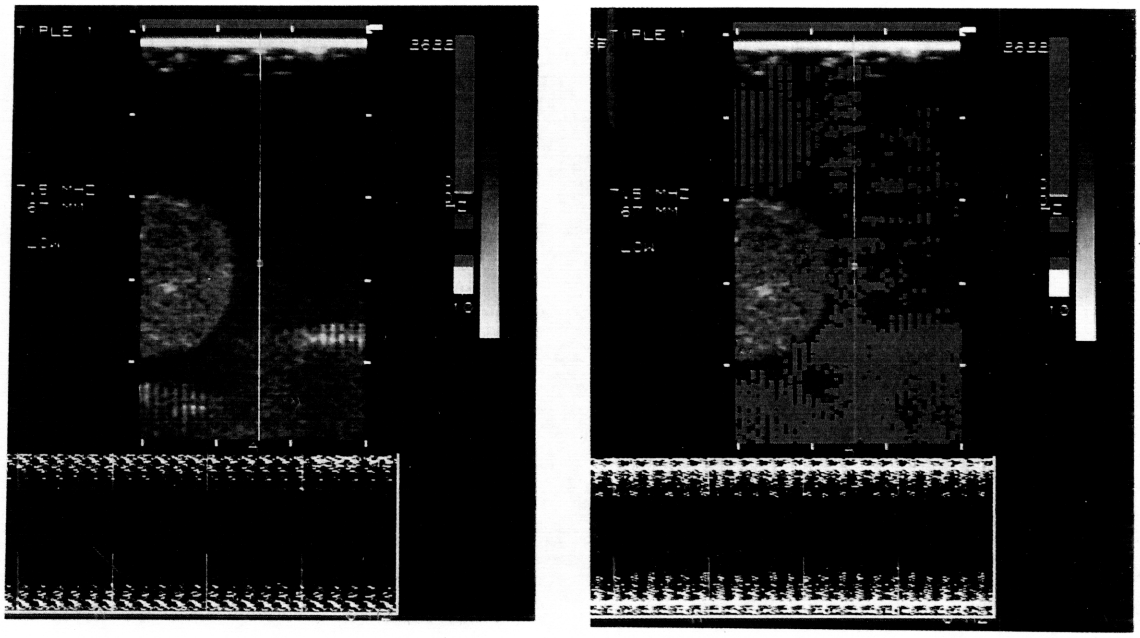

(a) (b)

Fig. 6. Images of a soft phantom containing a cylindrical "hard tumor." (a) B-scan image of hyperechoic cylindrical (cross section) at mid-left. (b) Sonoelasticity image shows vibration localized in the soft medium.

tween anechoic stand-off pads. Hypoechoic necrotic areas were surrounded by palpably stiff perimeters. Figure 7(b) shows the Doppler color image at modest vibrational amplitudes. Note the fill-in of surrounding tissue and between stiff perimeters. Again, in real-time the frame-by-frame color consistency (or

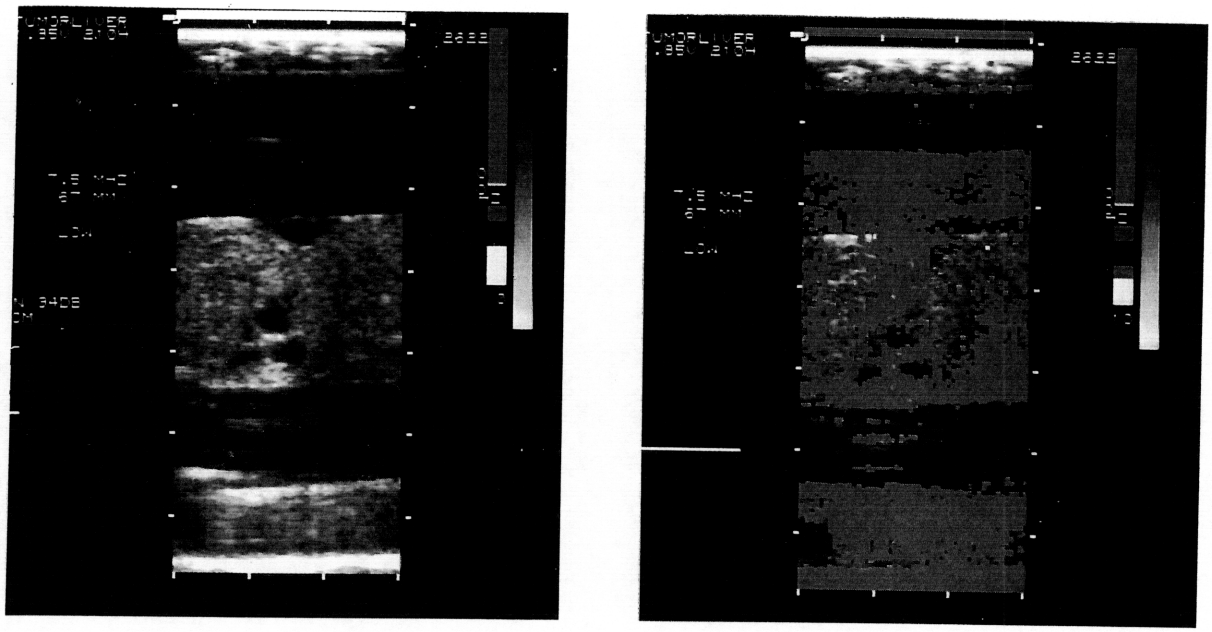

(a) (b)

Fig. 7. Images of rabbit liver (*in vitro*) containing VX2 tumor (1.5 cm). (a) B-scan image shows the tumor periphery is nearly isoechoic with the normal liver parenchyma (extreme right and left). (b) Sonoelasticity image shows fill-in occurs in all regions except for the stiff tumor periphery and the necrotic areas.

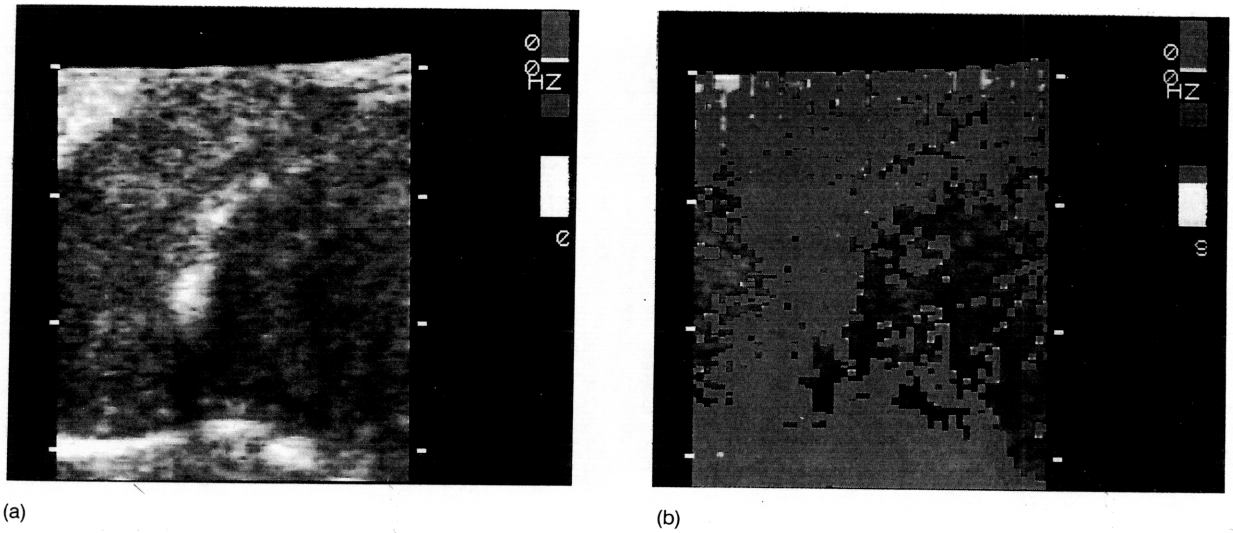

(a) (b)

Fig. 9. One quadrant images in transverse cross-section of an autopsy prostate specimen from an 80 year old male with benign prostatic hypertrophy. (a) B-scan image shows the inner gland (slightly hypoechoic lower central right) and peripheral zone (bottom left to top left and towards top right). (b) the sonoelasticity image shows demarcation of zones with greater vibration detected in the peripheral zone.

lack thereof in tumor perimeters) added to the discrimination between regions.

Figure 8(a) shows a smaller VX2 tumor (than in Fig. 7a), with no necrotic area and nearly isoechoic speckle compared to the surrounding rabbit liver. The cone of the acoustic vibration source can be seen near the bottom of the image. The vibration source on low amplitude in Figure 8(b) and higher in Fig. 8(c), gives progressive color fill-in, representing detection of vibrations above a fixed threshold. Note

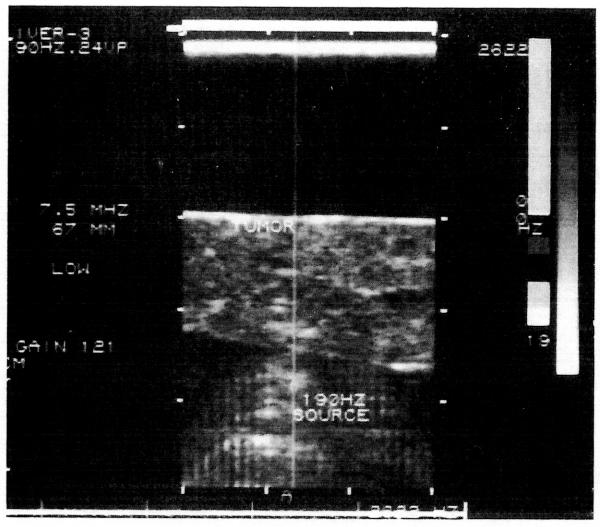

(a)

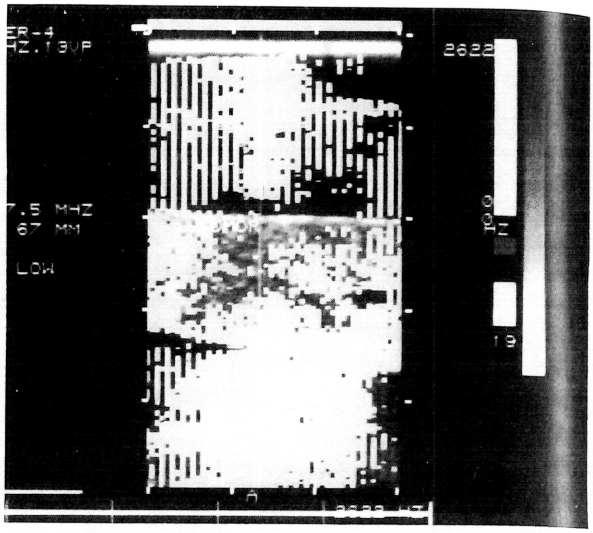

(b)

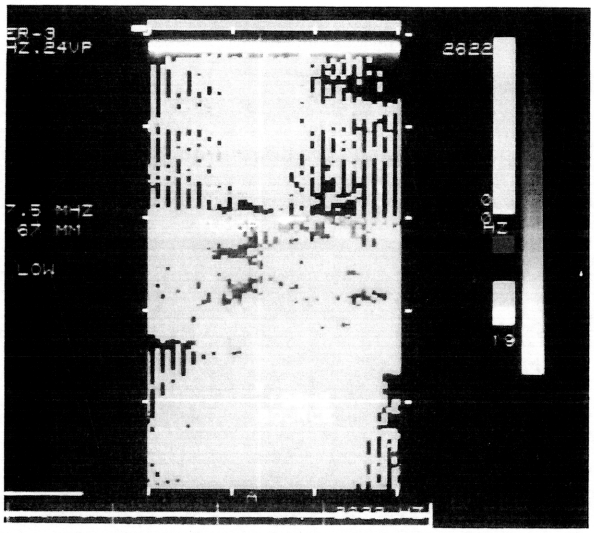

(c)

Fig. 8. Images of rabbit liver (*in vitro*) containing VX2 tumor (7 mm) with no necrotic area and nearly isoechoic with surrounding rabbit liver tissue. (a) The B-scan image shows the 190 Hz vibration source at bottom, and the tumor location indicated by the label. (b) With the source on low amplitude, the tumor region has minimal fill-in. (c) With source amplitude increased by a factor of 2, greater fill in of detected vibration occurs, but not the central tumor. The stiffness effect is perhaps aided by desmoplastic reactions in the surrounding tissues.

that the tumor region is the last to fill-in. In this case, the sonoelasticity image compared favorably to the location and extent of the palpably stiff region.

One quadrant of an *in-vitro* B-scan image of a whole prostate autopsy specimen from an 80-year-old male with benign prostatic hypertrophy is shown in Fig. 9(a). The sonoelasticity image, Fig. 9(b) demonstrates higher vibration in the perpheral zone than in the inner gland (lower-right) region of benign hypertrophy. This points to the need of further understanding of how source and object geometry, stiffness and boundary conditions all interact to produce a sonoelasticity image.

DISCUSSION

The idea of characterizing tissue from motion or mechanical response is not new but has had only limited evaluation (Dickenson and Hill 1982; Eisensher et al. 1983; Gore et al. 1979; Rockoff et al. 1978; Tristam et al. 1986, 1988; Wilson and Robinson 1982). Ultrasound detection schemes have utilized correlations between A-lines to detect motion of cardiovascular origin, and visual analysis of M-mode waveforms have been performed to detect motion for a 1.5 Hz external vibration source. These techniques have not reached clinical maturity because of a number of difficulties. The A-line or M-Mode techniques rely primarily on echoes from speckle regions, with few discrete specular reflections available to demonstrate motion unequivocally. The changes in speckle pattern resulting from motion of the sample volumes are complex and can be difficult to interpret. The correlations may suffer from patient motion caused by respiration and other body movements. The use of

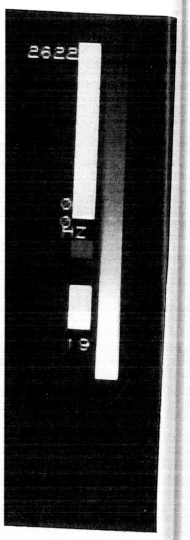

cardiovascular pulses to generate internal motion is problematic because the "source function," the radial expansion of arteries, is not a controllable parameter in terms of vibration rate and displacement profile applied to the target tissue.

In comparison, the approach embodied in the present research employs a variable frequency, external, vibration source and incorporates color coded Doppler ultrasound to detect the periodic movements of tissues. The use of Doppler and applied vibrations to characterize tissue elasticity has been independently explored by Levinson and colleagues (Levinson 1987; Kroukop et al. 1987) and Yamakoshi et al. (1988). The advantages of our technique derive from the known frequency of the applied stimulus, which can be used in estimation algorithms to reject other forms of motion such as respiration. Also, since the Doppler signal is capable of resolving small (tens of microns) oscillations, the response of deep tissues can be measured. Furthermore, the vibration frequency can be adjusted to take advantages of the low frequency properties of tumors and tissues (Parker et al. 1990).

As a result of these advantages, the combined external vibration and Doppler ultrasound detection approach appears to be the leading candidate for imaging the relative elastic properties of discrete regions of tissue, which may facilitate detection of tumors and other focal abnormalities in soft tissue.

Major unanswered questions remain concerning the best method for estimating local vibration amplitudes from the observed harmonics. More knowledge of the mechanical properties of normal and pathological tissues is required, along with optimization of the vibrational source in order to discriminate between layered, soft tissues, and hard inclusions.

Acknowledgments—The authors are grateful for the advice and insight of Dr. R. Gramiak, Dr. J. Holen, and Professor R. C. Waag. This work was supported by the Departments of Electrical Engineering and Radiology during an era when many funding agencies were pursuing their own agendas.

REFERENCES

Burks, D. D.; Fleischer, A. C.; Liddell, H.; Kulkarni, M. V. Transrectral prostate sonography: Evaluation of sonographic features in benign and malignant disease. Radiology 149:265–271; 1983.

Carlson, A. B. Exponential modulation. In: Carlson, A. B., ed. Communications systems. New York: McGraw Hill; 1986:221–271.

Censor, D. Acoustical Doppler effect analysis—Is it a valid method? J. Acoust. Soc. Am. 83(4):1223–1230; 1988.

Dickenson, R. J.; Hill, C. R. Measurement of soft tissue motion using correlation between A-scans. Ultrasound Med. Biol. 8:263–271; 1982.

Eisensher, A.; Schweg-Toffler, E.; Pelletier, G.; Jacquemard, G. La palpation échographique rythmée—Echosismographie. J. Radiol. 64:225–261; 1983.

Gore, J. C. Dynamic autocorrelation analysis of A-scans, in ultrasonic tissue. In: Linzer, M., ed. Tissue char. II, NBS special publ., Vol. 525:1979;275–280.

Hermand, J. P.; Lerner, R. M.; Huang, S. R.; Parker, K. J. Doppler shift techniques for speed of sound measurements and sonoelasticity images. 13th International Symposium on Ultrasonic Imaging and Tissue Characterization, June 6–8, 1988, Arlington, VA. New York: Academic Press, Inc.

Holen, J.; Waag, R. C.; Gramiak, R. Representations of rapidly oscillating structures on the Doppler display. Ultrasound Med & Biol. 11:267–272; 1985.

Kroukop, T. A.; Dougherty, D. R.; Levinson, S. F. A pulsed Doppler ultrasonic systems for making noninvasive measurements of the mechanical properties of soft tissue. J. Rehabil. Res. Dev. 24:1–8; 1987.

Lerner, R. M.; Parker, K. J. Sono-elasticity imaging. In: Kessler, L. W., ed. Acoustic imaging. New York: Plenum Co.; 1988:317–327.

Lerner, R. M.; Parker, K. J. Sono-elasticity in ultrasonic tissue characterization and echographic imaging. In: Thyssen, J. M., ed. Proceedings of the 7th European Communities Workshop, October, 1987, Nijmegen, The Netherlands. Luxembourg: European Communities.

Levinson, S. F. Ultrasound propagation in anisotropic soft tissues: The application of linear elastic theory. J. Biomech. 20:251–260; 1987.

Parker, K. J.; Huang, S. R.; Musulin, R. A.; Lerner, R. M. Tissue response to mechanical vibrations for "sonoelasticity imaging." Ultrasound Med Biol. 16:241–246; 1990.

Piquette, J. C.; Van Buren, A. L.; Rogers, P. H. Censor's acoustical Doppler effect analysis—Is it a valid method? J. Acoust. Soc. Am. 83(4):1681–1682; 1988.

Rifkin, M. D.; Kurtz, A. B.; Choi, H. Y.; Goldberg, B. B. Endoscopic ultrasonic evaluation of the prostate using a transrectal probe: Prospective evaluation and acoustic characterization. Radiology 149:265–271; 1983.

Rockoff, S. D.; Green, R. C.; Lawson, T. L.; Pett, S. D., Jr.; Devine III, D.; Francisco, S. G. Noninvasive measurement of cardiac pressures by induced ventricular wall resonance: Preliminary results in the dog. Investigative Radiology 13:499–505; 1978.

Tristam, M.; Barbosa, D. C.; Cosgrove, D. O.; Nassiri, D. K.; Bamber, J. C.; Hill, C. R. Ultrasonic study of in-vivo kinetic characteristics of human tissues. Ultrasound Med. Biol. 12:927–937; 1986.

Tristam, M.; Barbosa, D. C.; Cosgrove, D. O.; Bamber, J. C.; Hill, C. R. Application of Fourier analysis to clinical study of patterns of tissue movement. Ultrasound Med. Biol. 14:695–707; 1988.

Wilson, L. S.; Robinson, D. E. Ultrasonic measurements of small displacement and deformations of tissue. Ultrasonic Imaging 4:71–82; 1982.

Yamakoshi, Y.; Mori, E.; Sato, T. Imaging of precise movement of soft tissue for forced vibration. (abstr.). In: Linzer, M., ed. 13th International Symposium on Ultrasonic Imaging and Tissue Characterization, June 6–8, 1988, Arlington, VA. New York: Academic Press, Inc.